

Materials Science Communication

Influence of the copper content on the electrical conductivity of amorphous semiconductors from the system CuAsSe

M. Domínguez*, E. Márquez, P. Villares, R. Jiménez-Garay

Department of Condensed Matter Physics, University of Cádiz, Faculty of Science, PO Box 40, E-11510 Puerto Real (Cádiz), Spain

Received 19 December 1994; accepted 1 May 1995

Abstract

The electrical conductivity of three glassy samples from the system CuAsSe and its variation with temperature have been studied. The d.c. conductivity has been obtained from the linear current–voltage measurements, showing an Arrhenius-type dependence on temperature. The pre-exponential factor in this dependence indicates that the electrical conduction takes place by hopping between localized states in the gap. This theoretical model also explains the rise in conductivity when the copper content is increased. The a.c. conductivity of the samples has been measured by means of a complex impedance spectroscopic method, in the range $1-10^5$ Hz, under isothermal conditions. From the real part of this parameter, the d.c. conductivity (frequency independent component) is also calculated. The frequency dependent component of a.c. conductivity fits adequately well to the Debye model. This fact implies that ionic conductivity is much lower than electronic conductivity in these materials, and the dielectric relaxation process shown has been explained in terms of the hopping model described for d.c. electrical conduction.

Keywords: Copper content; Hopping model; Isothermal conditions

1. Introduction

Metal-chalcogenide glasses are an interesting type of semiconductor, since the presence of d-transition metals inside the amorphous chalcogenide lattice induces some appreciable changes in their electrical and other physical properties [1]. For example, in the case of copper-chalcogenide glasses, it has been shown that the evolution from low average coordination number materials (≥ 3) to nearly tetrahedral compounds results in the appearance of medium range order [2]. Additionally, the electrical conductivity increases with copper content increasing, as a result of the higher metallic character of the alloy [3]. This type of glassy system has shown some experimental evidence of ionic conduction (especially those containing silver), which could occur by thermally activated diffusive motion of metallic ions [4]. The study of the electrical

properties of these compounds could shed some light on the interesting process of photo-activated diffusion of metals in thin films of binary chalcogenide glassy alloys.

2. Experimental

The glassy alloys, of the nominal composition $\text{Cu}_x\text{As}_{50-x}\text{Se}_{50}$ (with $x = 5, 10$ and 20 at.%, named as CAS-5, CAS-10 and CAS-20, respectively, in the rest of the text), were obtained by the usual melt-quench method [5]. The non-crystalline nature of the samples was checked by X-ray diffraction [6] and differential scanning calorimetry [7]. Additionally, the final composition of the alloys was also checked by atomic absorption analysis [5].

For the electrical measurements, the ingots obtained in the quenching process were cut into ≈ 5 mm thick slices, which were then embedded into an epoxy-type resin. The sample parallel faces were polished until

* Corresponding author.

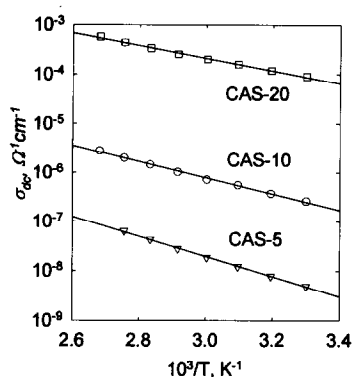
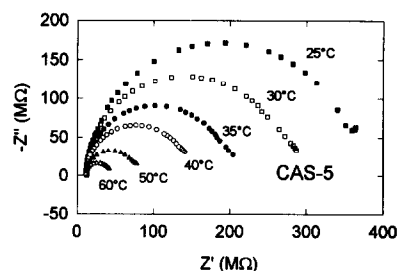


Fig. 1. Semilogarithmic plot of conductivity of the three alloys vs. inverse temperature.

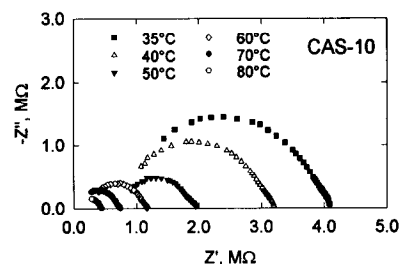
mirror-like surfaces were obtained, to ensure a good electrical contact with the electrode system. These electrodes were made of graphite paint, which was sprayed over the surfaces of the samples. The whole system was put into a furnace at 60 °C to accelerate drying of graphite paint, while monitoring the electrical resistance of the samples to check their total dryness (this point was detected by the constant electrical resistance). To carry out the electrical measurements at variable temperature, the samples were introduced inside a furnace whose temperature was continuously controlled by a PID-type temperature controller. All the electrical measurements were done in the dark. The d.c. electrical measurement system has already been fully described elsewhere [5], while the a.c. experiments were carried out with a lock-in amplifier (EG & G model 3210), in the range of frequencies 1–10⁵ Hz. The complex electrical impedance of the samples was obtained by simultaneously measuring the complex voltage applied to the sample and the complex voltage drop at a fixed resistor in series with the sample. The nominal value of this resistor was always below 0.1% of the sample resistance at d.c. conditions. To avoid the influence of Joule self-heating during the experiments, the amplitude of the a.c. applied voltage was kept at 1 V. All the measurements were corrected from the circuit impedance (series and parallel) by measuring the short-circuit and open-circuit impedance.

Table 1
Parameters found in the fit of experimental data to Eq. (1)

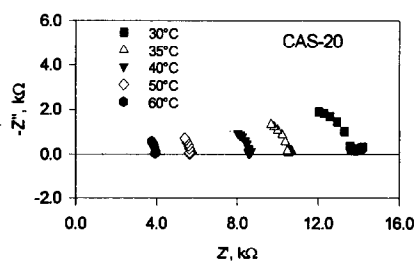
	CAS-5	CAS-10	CAS-20
$\sigma_0, \Omega^{-1} \text{cm}^{-1}$	4.8×10^{-2}	1.7×10^{-1}	2.7
$\Delta E, \text{eV}$	0.42	0.36	0.27
$\sigma_{298 \text{ K}}, \Omega^{-1} \text{cm}^{-1}$	3.2×10^{-9}	1.7×10^{-7}	6.5×10^{-5}
r	0.9998	0.994	0.994



(a)



(b)



(c)

Fig. 2. Complex impedance plots for the three alloys under study: (a) CAS-5; (b) CAS-10; (c) CAS-20.

3. Results and discussion

3.1. D.c. electrical conductivity

The conductivity of the samples, under d.c. conditions, was calculated from the linear I – V characteristics, considering their geometric factors. Fig. 1 shows the plots of the electrical conductivity versus the inverse of the temperature, on a semilogarithmic scale. The experimental data fit to the known Arrhenius-type dependence [5]:

$$\sigma = \sigma_0 \cdot \exp\left(\frac{-\Delta E}{k_B T}\right) \quad (1)$$

where σ_0 is the pre-exponential factor, ΔE is the activation energy for this thermally activated process, and k_B is the Boltzmann constant. From least squares analysis, the values for both fitting parameters for each copper-chalcogenide alloy were found. These values are shown in Table 1.

The pre-exponential factor increases, along with the conductivity, when the copper content increases, while the activation energy decreases. The increase in the

electrical conductivity can be explained in terms of the density of defects inside the amorphous lattice. The addition of copper, and of d-elements in general, to chalcogenide glasses makes the concentration of bond defects increase. These defects are the main factor responsible for electrical conduction in this kind of amorphous semiconductor, which takes place by hopping of carriers (holes in this case), between localized energy levels in the gap. Additionally, the decrease in the activation energy has been interpreted as a consequence of the shift of the Fermi level towards the conduction band, due to the existence of a higher number of defects when the copper content is increased [5].

3.2. Complex impedance spectroscopic analysis

The complex impedance of the samples is calculated from the voltage drop at the series resistor, from the expression

$$\frac{V^*}{R + Z_s^*} = \frac{V_R^*}{R} \quad (2)$$

where V^* is the complex applied voltage (taken as the reference for the phase measurements), R is the fixed resistor value, Z_s^* is the sample complex impedance, and V_R^* is the complex voltage drop at the fixed resistor, measured by the lock-in amplifier and corrected for circuit impedance as aforementioned.

Fig. 2 shows the complex impedance plots of the samples under study, for different ambient temperatures. In all cases, the experimental data appear as one or two slightly flattened semicircles, whose centers lie slightly below the real axis. This kind of behavior has been generally called ‘non-Debye’, as opposed to those solid electrolytes showing a regular semicircle centered on the real axis (Debye-type behavior). Nevertheless, in this case, the deviations are very low and the expressions derived from the Debye model fit adequately well to the experimental results.

The lower frequency semicircles, which in some cases are only a simple dispersion of data, are attributed to the double-layer polarization at the electrode interface, as pointed out by McDonald [8] and Bauerle [9]. In the case of the higher-copper-content alloy, this low frequency semicircle is the only one which appears, and the study is thus very restricted. It would be necessary to increase the frequency of the applied signal to obtain the second semicircle.

The experimental data can be fitted to several phenomenological relationships. For example, the characteristic parameters of the different semicircles (radius and center complex coordinates) can be obtained, and their evolution with temperature and sample composition can be studied. Bearing this idea in mind, the experimental results were fitted to the expression

Table 2
Results of the non-linear fitting to the equivalent circuit model

	$T, ^\circ\text{C}$	R_{ohm}, Ω	R_p, Ω	C_p, F
CAS-5	30	1.19×10^7	2.67×10^8	2.01×10^{-11}
	50	1.15×10^7	6.77×10^7	1.57×10^{-11}
	80	1.11×10^7	1.69×10^7	1.44×10^{-11}
CAS-10	30	9.16×10^5	4.42×10^6	4.10×10^{-11}
	50	6.04×10^5	1.03×10^6	1.18×10^{-10}
	80	1.12×10^4	3.24×10^5	6.58×10^{-11}
CAS-20	30	9.09×10^3	4.59×10^3	4.81×10^{-10}
	40	5.17×10^3	2.78×10^3	8.34×10^{-11}
	60	2.11×10^3	1.85×10^3	1.31×10^{-12}

$$-Z'' = -Z'_C + \sqrt{r^2 - (Z' - Z'_C)^2} \quad (3)$$

where (Z', Z'') are the real and imaginary parts of the sample complex impedance, (Z'_C, Z''_C) are the complex coordinates of the center, and r is the radius of the semicircle. From these values, the intersection points with the real axis can also be obtained (R_{LF} and R_{HF} , i.e., the resistance at low and high frequencies, respectively). Alternatively, the phenomenological model of the equivalent circuit can also be considered. The electrical response of the samples in the frequency domain can be simulated by that of a simple circuit, made of a combination of resistors and capacitors. Several equivalent circuits were checked with our data, but the one to which these results are best fitted is made of two parallel RC circuits in series with an additional resistor. The first parallel RC circuit represents the polarization at the electrode interface, while the second is related to the bulk relaxation. Finally, the additional resistor in series with these RC circuits, commonly known as ohmic resistance, explains the saturation of conductivity at high frequencies.

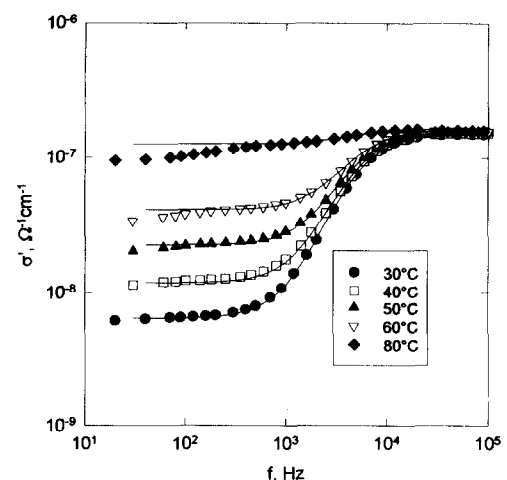


Fig. 3. Electrical conductivity of sample CAS-5 as a function of frequency, at different temperatures.

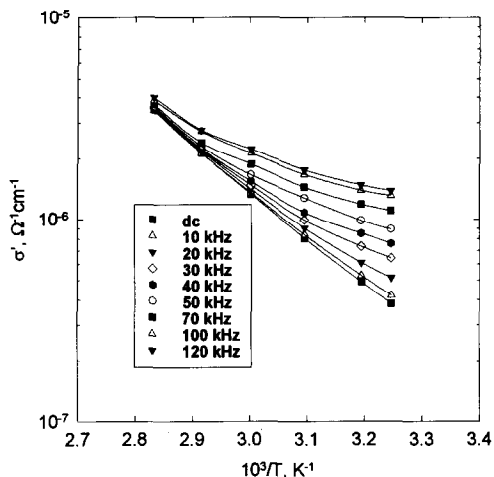


Fig. 4. A.c. electrical conductivity of sample CAS-10 vs. inverse temperature, at different frequencies.

Table 2 shows the results obtained for these fit parameters. It may be concluded that the capacitive component of the samples decreases faster than the resistive one when the temperature is increased, i.e., the dielectric relaxation effect is less important as the temperature is raised. Nevertheless, it should be noticed that all the fit parameters decrease with temperature, as a result of the semiconductor behavior of the glassy alloys.

3.3. The a.c. electrical conductivity

From the values of the complex impedance previously discussed, it is possible to calculate the complex electrical conductivity of the samples under study, by means of the relationship

$$\sigma^* = \frac{d}{S} (Z^*)^{-1} \quad (4)$$

where d is the interelectrode distance and S is the electrode surface area. The real conductivity thus obtained, $\sigma'(\omega)$, can be separated into two components, one of them dependent and the other independent of frequency:

$$\sigma(\omega) = \sigma_{\text{d.c.}} + \sigma_{\text{a.c.}}(\omega) \quad (5)$$

The experimental results for the real conductivity of sample CAS-5 have been plotted versus the frequency, on a log–log scale, for different ambient temperatures, as shown in Fig. 3. Furthermore, the equivalent data for sample CAS-10 has also been plotted versus inverse temperature at different frequencies in Fig. 4. It may be concluded from this plot that the electrical conductivity depends linearly on inverse temperature when the frequency is low (i.e., near d.c. conditions), but diverges from this behavior as the frequency increases. At the highest available frequencies, the conductivity is almost constant with tempera-

Table 3

Parameters obtained in the non-linear fits of experimental results of electrical conductivity, for two of the samples, to Eq. (6)

	$T, ^\circ\text{C}$	$\sigma_{\text{sat}}, \Omega^{-1} \text{cm}^{-1}$	τ, s
Sample CAS-5	30	1.42×10^{-7}	3.26×10^{-5}
	50	1.34×10^{-7}	3.06×10^{-5}
	60	1.29×10^{-7}	3.04×10^{-5}
	80	1.19×10^{-7}	2.98×10^{-5}
Sample CAS-10	35	1.26×10^{-6}	2.66×10^{-6}
	40	1.37×10^{-6}	2.60×10^{-6}
	60	2.78×10^{-6}	1.93×10^{-6}
	80	3.75×10^{-6}	8.92×10^{-7}

ture. This behavior has also been shown by other types of materials [10].

These results have been fitted to the known Debye model for dielectric relaxation, from which the real part of the complex electrical conductivity is given by

$$\sigma_{\text{a.c.}}(\omega) = \sigma_{\text{sat}} \cdot \frac{\omega^2 \tau^2}{1 + \omega^2 \tau^2} \quad (6)$$

where τ is the relaxation time. Table 3 shows the results of the non-linear fit to this type of dependence. Additionally, the lines shown in Fig. 3 correspond to the different Debye-like functions fitted to the experimental results.

4. Conclusions

The electrical characterization, under both d.c. and a.c. conditions, of glassy semiconducting alloys from the metal-chalcogenide system $\text{Cu}_x\text{As}_{50-x}\text{Se}_{50}$ has been carried out, at ambient temperatures in the range 25–100 °C. The d.c. conductivity shows the typical Arrhenius-type dependence on temperature. This behavior is explained in terms of the hopping conduction mechanism. On the other side, the a.c. conductivity fits adequately well to the known Debye model for dielectric relaxation. This fact implies that the contribution of ionic conductivity to the total conduction mechanism in a.c. conditions must be low. The electronic conduction mechanism of hopping between localized states in the gap also explains this behavior adequately well.

References

- [1] B. T. Kolomiets, Y. V. Rhukyladev and V. P. Shilo, *J. Non-Cryst. Solids*, 5 (1971) 402.
- [2] Z. M. Zaleh, G.A. Williams and P. C. Taylor, *J. Non-Cryst. Solids*, 137/138 (1991) 1047.

- [3] A. V. Danilov and E. Mosli, *Sov. Phys. Solid State*, 5(1963) 1472.
- [4] E. Márquez, R. Jiménez-Garay, A. Zakery, P.J.S. Ewen and A.E. Owen, *Philos. Mag. B*, 63 (1991) 1169.
- [5] M. Domínguez, E. Márquez, P. Villares and R. Jiménez-Garay, *Mater. Lett.*, 19 (1994) 69.
- [6] J. Vázquez, M. Domínguez, P. Villares and R. Jiménez-Garay, *J. Phys. Chem. Solids*, 52 (1991) 567.
- [7] R. Ligeró, J. Vázquez, P. Villares and R. Jiménez-Garay, *Thermochim. Acta*, 157 (1990) 181.
- [8] J. R. MacDonald, *J. Chem. Phys.*, 61 (1974) 3977.
- [9] J. E. Bauerle, *J. Phys. Chem. Solids*, 30 (1969) 2657.
- [10] A. K. Jonscher, *J. Non-Cryst. Solids*, 8-10 (1972) 293.